



Published in final edited form as:

Cancer Res. 2016 February 1; 76(3): 582–593. doi:10.1158/0008-5472.CAN-15-1199.

Aberrant activation of Notch signaling inhibits PROX1 activity to enhance the malignant behavior of thyroid cancer cells

Dongwon Choi¹, Swapnika Ramu¹, Eunkyung Park¹, Eunson Jung¹, Sara Yang¹, Wonhyeuk Jung¹, Inho Choi^{1,2}, Sunju Lee¹, Kyu Eui Kim¹, Young Jin Seong¹, Mingu Hong¹, George H. Daghljan¹, Daniel Kim¹, Eugene Shin¹, Jung In Seo¹, Vicken Khatchadourian¹, Mengchen Zou³, Wei Li³, Roger E. De Filippo⁴, Paul J. Kokorowski⁴, Andy Y. Chang⁴, Steve S. Kim⁴, Ana Santin⁵, Tania Furlanetto⁶, Sung S. Shin⁷, Meng Li⁸, Yibu Chen⁸, Alex K. Wong¹, Chester J. Koh⁹, Jan Geliebter¹⁰, and Young-Kwon Hong¹

¹Division of Plastic and Reconstructive Surgery, Department of Surgery, Norris Comprehensive Cancer Center, Keck School of Medicine, University of Southern California, Los Angeles, California

²Department of Pharmaceutical Engineering, College of Life and Health Sciences, Hoseo University, Asan, Chungnam, Republic of Korea

³Department of Dermatology, Norris Comprehensive Cancer Center, Keck School of Medicine, University of Southern California, Los Angeles, California

⁴Division of Urology Children's Hospital Los Angeles and Department of Urology Keck School of Medicine University of Southern California

⁵Department of Basic Health Sciences, Federal University of Health Sciences of Porto Alegre, RS, Brazil

⁶PostGraduation Program in Medicine: Medical Sciences, Federal University of Rio Grande do Sul, Porto Alegre, RS, Brazil

⁷Department of Pathology, Kaiser Permanente Medical Center, Fontana, California

⁸Bioinformatics Service Program, Norris Medical Library, University of Southern California

⁹Division of Pediatric Urology, Texas Children's Hospital, Baylor College of Medicine, Houston, Texas

¹⁰Department of Microbiology & Immunology, Department of Otolaryngology, New York Medical College, Valhalla, New York

Correspondence should be addressed to: Young-Kwon Hong, Ph.D., Department of Surgery, University of Southern California, Norris Comprehensive Cancer Center, 1450 Biggy St. NRT6501, Los Angeles, CA 90033, Tel: 323-442-7825, young.hong@usc.edu. Dongwon Choi, Swapnika Ramu and Eunkyung Park contributed equally to this study.

The authors declare no financial interests with this study.

AUTHOR CONTRIBUTION

D.C., S.W., E.P., E.J., S.Y., W.J., I.C., S.L., K.K., Y.S., M.H., G.D., D.K., E.S., J.S., V.K., M.Z., A.S. have participated in and/or performed the experiments. M.L., Y.C., S.S., T.F., A.W., J.G., Y.H. analyzed the data. R.E., P.K., A.C., S.K., W.L., A.W., C.K., J.G. supplied materials. T.F., A.W., W.L., J.G., Y.H. supervised and designed the study. A.W., J.G., Y.H. wrote, reviewed and revised the article.

Abstract

Papillary thyroid cancer (PTC) is one of the most common endocrine malignancies associated with significant morbidity and mortality. Although multiple studies have contributed to a better understanding of the genetic alterations underlying this frequently arising disease, the downstream molecular effectors that impact PTC pathogenesis remain to be further defined. Here, we report that the regulator of cell fate specification, PROX1, becomes inactivated in PTC through mRNA downregulation and cytoplasmic mislocalization. Expression studies in clinical specimens revealed that aberrantly activated NOTCH signaling promoted PROX1 downregulation and that cytoplasmic mislocalization significantly altered PROX1 protein stability. Importantly, restoration of PROX1 activity in thyroid carcinoma cells revealed that PROX1 not only enhanced Wnt/ β -catenin signaling, but also regulated several genes known to be associated with PTC, including thyroid cancer protein (TC)-1, SERPINA1, and FABP4. Furthermore, PROX1 re-expression suppressed the malignant phenotypes of thyroid carcinoma cells, such as proliferation, motility, adhesion, invasion, anchorage-independent growth, and polyploidy. Moreover, animal xenograft studies demonstrated that restoration of PROX1 severely impeded tumor formation and suppressed the invasiveness and the nuclear/cytoplasmic ratio of PTC cells. Taken together, our findings demonstrate that NOTCH-induced PROX1 inactivation significantly promotes the malignant behavior of thyroid carcinoma, and suggest that PROX1 reactivation may represent a potential therapeutic strategy to attenuate disease progression

Keywords

Papillary Thyroid Cancer; PROX1; NOTCH; Wnt; Endocrine Malignancies

INTRODUCTION

Thyroid carcinoma is one of the most common and fast rising endocrine malignancies with significant morbidity and mortality over past decades. Subtypes of thyroid carcinoma include well-differentiated papillary and follicular forms, with a gradual progression to the more undifferentiated anaplastic thyroid carcinoma. In recent years, the incidence of thyroid carcinoma has been rising steadily, largely due to increased diagnoses of the papillary variant of this disease (1). Approximately 80% of all thyroid cancers diagnosed in the United States are papillary thyroid cancer (PTC). Surgical resection along with radioactive iodine treatment is currently the principal procedure in management of PTC. While PTC responds very well to surgical and therapeutic intervention, a small subset of tumors progress to undifferentiated anaplastic type and become extremely aggressive with a significantly decreased survival rates.

The genetic events underlying the initiation and progression of PTCs have been extensively studied and most of these alterations result in increased activation of the mitogen-activated protein kinase (MAPK) signaling pathway. One such mechanism is through chromosomal rearrangements giving rise to the chimeric oncogene RET/PTC, where the C-terminal kinase domain of the RET transmembrane tyrosine kinase receptor is fused to one of a number of possible upstream partners, resulting in its constitutive activation. Another common genetic alteration is mutations in the BRAF gene, typically a V600E gain-of-function mutant form

of the BRAF protein. Constitutive activation of the AKT pathway has also been reported in PTCs.

In this study, we demonstrate that *PROX1* mRNA expression was decreased in thyroid cancer specimens compared to adjacent normal tissues, and that activated NOTCH signaling was identified as the causative mechanism. Interestingly, PROX1 protein was mislocalized to the cytoplasm and gained increased protein stability. When PROX1 function was restored in PTC, it profoundly suppressed not only the expression of genes whose expression has been associated with thyroid cancer development, but also the malignant phenotypes of thyroid carcinoma *in vitro* and *in vivo*. Together, we conclude that inactivation of PROX1 activity, through transcriptional downregulation and/or protein mislocalization, profoundly contributes to the carcinoma phenotypes and may represent an essential event in thyroid cancer development.

METHODS

Reagents, Cell Cultures and Tissue RNA Samples

BCPAP, TPC1 and 8508c cells were authenticated by the University of Arizona Genetics Core. BCPAP-Ctr and BCPAP-Prx cell were generated as follows. BCPAP cells were infected with rTTA2 or empty lentivirus (from Dr. Wange Lu, University of Southern California) and transfected either with pIRES-hygromycin vector (Clontech) to generate BCPAP-Ctr cells, or with Flag-*PROX1*-IRES-hygromycin vector to make BCPAP-Prx cells. Two representative clones were chosen for further studies. PROX1 expression was induced with 0.5 µg/ml doxycycline (Dox) for 48 hours. RNA sequencing data using BCPAP-Ctr and BCPAP-Prx cells were deposited in Gene Expression Omnibus (GEO) (Accession No. GSE75059). PROX1-expressing TPC1 and 8508c stable cells were generated by transfecting each cell line with pcDNA3 or pcDNA3-Flag-*PROX1*, followed by G418-based selection. After 3 weeks, multiple colonies of G418-resistant cells were pooled together for further expansion and studies. RNAs from PTC (GSE3678) and goiter nodule tissues (2) were previously described.

Cell Behavior Assays

5-Bromo-2'-deoxyuridine (BrdU, Sigma-Aldrich Co.) -mediated proliferation assay was performed as previously (3). Cell motility was determined by allowing cells to move on the colloidal gold-covered surface and measuring their migrated tracks, as previously described (4). Monolayer scratch assay was performed as previously described (5). Invasive phenotype was measured as previously described (6). The anchorage independent growth assay was performed in soft agar as previously described (7).

Analysis of Gene Expression Database

We performed the comparative analyses of gene expression profiles using various web-based bioinformatics tools. To retrieve and extract the deposited expression data and to systematically integrate and interpret the datasets, the Oncomine integrated data mining platform (www.oncomine.org) (8), NextBio Disease Atlas (www.nextbio.com) (9) and Gene Expression Omnibus (GEO) statistical tool (<http://www.ncbi.nlm.nih.gov/geo/>) were

reciprocally employed. Subsequently, computational analyses for the functional relationships were carried out using Ingenuity Pathway Analysis (IPA) (www.ingenuity.com).

Immunohistochemistry, Fractionation and Western Blotting Assay

Thyroid tissue microarray was purchased from Cybrdi, Inc. (Rockville, MD). Tissue sections were deparaffinized by successive washes in xylene and decreasing concentrations of ethanol from 100% to 70%. Antigen retrieval was performed by immersing slides in boiling sodium citrate buffer (pH) for 20 minutes, followed by quenching of endogenous peroxidase activity using 0.1% hydrogen peroxide in methanol. WTBS solution (Triton X-100, BSA goat serum in TBS) was used for blocking and antibody incubations. Sections were incubated with primary antibody overnight at 4 °C, followed by washing in TBS and incubation in secondary antibody for 30 min at RT. PROX1 antibodies used were obtained from ReliaTech GmbH and Covance Inc. Cycloheximide treatment of cells was carried out by treating cells with 100 µg/ml of cycloheximide (Sigma-Aldrich Co.), followed by preparation of whole cell lysate or fractionation as described above. Samples were then boiled in western loading buffer and separated by SDS-PAGE. The source of antibodies used for western blotting analyses were PROX1 (EMD Millipore), actin (Sigma-Aldrich Co), tubulin and lamin (Santa Cruz Biotech, Inc).

Tumor Graft Study

Animal experiments have been pre-approved by the University of Southern California Institutional Animal Care and Use Committee (IACUC). Tumor growth studies were performed as described previously (10). Briefly, three million BCPAP-Ctr and BAPAP-Prx cells were subcutaneously injected into the left and right back skin area of NOD-SCID IL2R γ null mice (the Jackson Laboratory). While mice in the control group (n = 4) were housed with normal drinking water, the treated group (n = 5) were provided with Dox-containing drinking water from day 1 (2 mg/mL in 5% sucrose water). After 28 days, tumors were harvested to measure their wet weights and analyzed for their histology.

Statistical Analysis

Student t-test (two-tailed) was used to determine whether the differences between the experimental and control groups were statistically significant. The analyses were performed using Microsoft Excel (Microsoft Office) and GraphPad PRISM6 (GraphPad Software, Inc).

More extensive details of experimental methods can be found in Supplemental Information.

RESULTS

PROX1 is downregulated in various types of thyroid carcinoma

Using the Oncomine integrated data mining platform (8), we performed a comprehensive analysis of PROX1 expression profiles in normal thyroid tissues versus various types of thyroid cancers (a total of 97 clinical samples including papillary, follicular and undifferentiated thyroid cancers) that were reported in a previous study (11). This analysis revealed that thyroid carcinoma cells show a consistent downregulation of PROX1 by more

than 2-fold ($p < 1E-4$) compared to normal thyroid tissues (Figure 1A). PROX1 downregulation in thyroid cancers was also confirmed using another set of thyroid cancer gene profiling study (Figure 1B) (12). Moreover, we performed analyses against additional public repositories (13–16) to investigate PROX1 expression through NextBio Disease Atlas (9) and consistently found PROX1 downregulation in various thyroid cancers (Figure 1C). Moreover, *PROX1* mRNA level was compared in PTCs vs. their adjacent normal tissues from the same patients using Gene Expression Omnibus (GEO) statistical tool against two independent data sets (GSE3467, GSE3678), which revealed PROX1 downregulation in PTCs relative to their matched normal tissues (Figure 1D,E). This finding was verified by quantitative real-time RT-PCR (qRT-PCR) (Figure 1F). Our expression analyses using GEO Data Set GSE27155 (11,17) showed that PROX1 expression was not affected by mutational status of BRAF and K/N/H-RAS genes or RET-PTC gene rearrangement. Notably, PROX1 downregulation can be already detectable in follicular adenomas and oncocyctic adenomas (Figure 1A), implying that this genetic event may happen in the early stage of follicular carcinogenesis. Therefore, we compared PROX1 expression between normal and goiter nodule tissues, but did not find any changes in PROX1 expression ($n=15$, Figure 1G). Together, our analyses found that PROX1 is consistently downregulated in various types of thyroid cancers.

Activated NOTCH signaling underlies PROX1 downregulation in thyroid cancer cells

We next set out to define the mechanism for PROX1 downregulation and asked whether PROX1 upstream regulators are also altered in the 133 clinical cancer samples collected from 3 independent studies (11,12,18) through a combined analysis using OncoPrint and Ingenuity Pathway Analysis (IPA), a web-based analysis tool for genomic data. In particular, we focused on two upstream regulators of PROX1, namely NOTCH and TGF- β pathways (19–21). Indeed, NOTCH downstream effectors HEY1 and HEY2, both of which have been identified as negative regulators of PROX1 (22), were upregulated in thyroid cancers with an integrated statistical significance of HEY1 ($p = 0.053$) and HEY2 ($p = 9.16E-4$) (Figure 2A). This finding is consistent with previous studies reporting activated NOTCH pathway in thyroid cancers (19–21). Upregulation of HEY1 and HEY2 is also supported by previous thyroid gene expression profiling studies (Supplemental Fig. 1A,B). Notably, the NOTCH ligand JAG2 was found to be upregulated ($p = 0.012$), while expression levels of the other NOTCH ligands (DLL1, DLL3, DLL4 and JAG1) and NOTCH receptors (NOTCH1–4) were not altered. In addition, analyses of GSE3678 revealed the upregulation of HEY2 in the 7 sets of PTC, compared to their adjacent normal tissues (Figure 2B). HEY1 upregulation was not found to be statistically significant in this set of samples. HEY2 upregulation in these matched clinical samples was further confirmed using qRT-PCR (Figure 2C). We then inhibited NOTCH receptors in a PTC cell line, BCPAP, using a γ -Secretase inhibitor DAPT or siRNA against NOTCH1, and found that PROX1 expression was concomitantly increased upon inhibition of NOTCH signaling (Figure 2D,E). In contrast, inhibition of TGF- β did not upregulate PROX1 in BCPAP (data not shown). We next knocked-down the expression of HEY1, HEY2 or both using siRNAs in BCPAP and TPC1. Whereas inhibiting either HEY1 or HEY2 alone did not alter PROX1 expression, a combined knockdown of both genes resulted in a synergistic upregulation of PROX1 (Figure 2F,G). Together, these data indicate that activated NOTCH pathway

underlies PROX1 downregulation in thyroid cancers and that HEY1 and HEY2 synergistically downregulate PROX1.

PROX1 protein is mislocalized to the cytoplasm with increased protein stability in thyroid cancer cells

We next performed immunohistochemistry (IHC) analyses against PROX1 using a thyroid cancer tissue array. Unexpectedly, while normal thyroid epithelial cells showed a clear nuclear staining of PROX1, most thyroid cancer cells showed both nuclear and cytoplasmic localization of PROX1 protein, and their PROX1 protein level did not reflect the above-demonstrated mRNA downregulation (Figure 3A). To address this discrepancy in PROX1 mRNA vs. protein levels, we first studied the subcellular localization of PROX1 protein in two different thyroid cancer cells, BCPAP and TPC1. An immortalized thyroid follicular epithelial cell line, Nthy-ori 3-1, was explored as a positive control for PROX1 localization, however, we failed to detect PROX1 in this cell line due to its low mRNA and protein expression. Instead, we employed human primary lymphatic endothelial cells (LECs) as a positive control for PROX1 nuclear localization. Indeed, our immunofluorescence (IF) assays using 4 different anti-PROX1 antibodies revealed that PROX1 protein was found mainly in the cytoplasm in BCPAP and TPC1 cells, whereas it is clearly localized to the nuclei of LECs (Figure 3B). Furthermore, we confirmed this data by separating the nuclear vs. cytoplasmic fractions from each cell type, followed by western blot analyses for PROX1 (Figure 3C).

While the nuclear export of *Drosophila* Prospero protein, a homologue of PROX1, was efficiently inhibited by leptomycin B, which blocks the exportin-mediated nuclear export, the cytoplasmic mislocalization of PROX1 in thyroid cancer cells was not affected by leptomycin B, sodium azide (ATP depletion) or low temperature (Supplemental Fig. 2). Interestingly, however, when we treated TPC1 cells with triiodothyronine (T3), the ligand for thyroid hormone receptor alpha (TR α), the cytoplasmic PROX1 signal increased, while the nuclear PROX1 signal correlatively diminished, resulting in a halo-like appearance of PROX1 staining (Supplemental Fig. 3).

Considering that PROX1 mRNA and protein levels did not correlate in thyroid cancers, we asked whether the PROX1 cytoplasmic mislocalization enhances its protein stability. To compare PROX1 protein stability, LECs, BCPAP and TPC1 cells were treated with cycloheximide, and their cell lysates were harvested at different time points to determine PROX1 level. Notably, PROX1 was much more stable in BCPAP and TPC1 cells than in LECs (Figure 3D,E). In addition, we compared protein stability between the cytoplasmic and nuclear PROX1 in TPC1 cells and found that cytoplasmic PROX1 was much more stable than nuclear PROX1 in TPC1 cells (Figure 3F,G). Together, our studies show that PROX1 was mislocalized to the cytoplasm in thyroid cancer cells and subsequently gained protein stability, which accounts for the discrepancy in levels of PROX1 mRNA versus protein.

Restored PROX1 expression significantly impacts transcriptional profiles of thyroid cancer cells

We investigated how PROX1 affects thyroid cancer gene expression profiles by restoring PROX1 expression in thyroid cancer cells. For this aim, we generated BCPAP cell lines that allow Doxycycline (Dox)-mediated inducible expression of PROX1 (BCPAP-Prx), along with corresponding control cell lines (BCPAP-Ctr). Western blot analyses confirmed that Dox treatment induced more than 10-fold overexpression of PROX1 in BCPAP-Prx cells, whereas endogenous PROX1 expression was not altered in BCPAP and BCPAP-Ctr cells (Supplemental Fig. 4A,B). With these PROX1-inducible cell lines, we evaluated the effect of restored PROX1 activity to the gene expression profiles of BCPAP cells. We first compared the gene expression profiles in PTCs vs. their neighboring normal tissues using two independent data sets, GSE3467 (n=9) (18) and GSE3678 (n=7), and identified 548 and 1,093 genes, respectively, that show > 2-fold changes ($p < 0.05$) in their expression. Next, we investigated how many of these genes are regulated by PROX1 by sequencing whole transcripts (RNA-Seq) from Dox-treated BCPAP-Prx and Dox-treated BCPAP-Ctr. This analysis revealed that PROX1 regulated 53 genes (9.6%) of the 548 genes for GSE3467, and 100 genes (9.1%) of the 1,093 genes for GSE3678 (> 2 fold changes) (Figure 4A).

Interestingly, our IPA analyses using GSE3467 and GSE3678 data sets unexpectedly found that Wnt/ β -catenin signaling is suppressed in the PTCs with statistically significant z-scores (-1.633 and -0.258, respectively) (Supplemental Fig. 5A,B). In particular, the Wnt/ β -catenin pathway genes that are found to be suppressed in PTCs compared to their matched normal cells include Frizzled receptors (FZD5, FZD8), Grouch proteins (TLE1, TLE4), Cadherin proteins (CDH1-3), TCF/LEF proteins (TCF4, TCF7L1) and Sox proteins (SOX4, SOX7, SOX9, SOX11) (Figure 4B,C). This finding was unexpected, but not inconsistent with previous reports, as Wnt/ β -catenin signaling has been implicated in the progression of various thyroid carcinoma (23). Therefore, we next assessed the impact of restored PROX1 activity to Wnt/ β -catenin signaling in BCPAP cells using the β -catenin reporter vector (TOP-Flash) and its negative control version (FOP-Flash) harboring mutations in the TCF/LEF binding site. We transiently introduced these reporter vectors into BCPAP-Ctr or BCPAP-Prx cells and treated them with Dox. Notably, PROX1 restoration activated the reporter activity up to 4-fold from TOP-Flash, but not FOP-Flash, selectively in BCPAP-Prx cells (Figure 4D), indicating that PROX1 enhances Wnt/ β -catenin signaling in BCPAP cells. In addition, PROX1 regulates several genes that were previously associated with thyroid cancer. For example, Thyroid Cancer (TC)-1 was originally isolated by its prominent expression in thyroid cancer cells (24,25) and known to promote G1/S cell cycle progression (26). While TC-1 was upregulated in PTCs, it was significantly downregulated by PROX1 re-expression (Figure 4E,F). SERPINA1 and CRABP1, two previously proposed diagnostic biomarkers for thyroid cancer (27), were also found to be strongly regulated by PROX1 (Figure 4E,F). Fatty acid binding protein 4 (FABP4) and TCF7L1, which were strongly downregulated in PTCs, were found to be upregulated upon PROX1 re-expression. Moreover, we engineered another PTC cell line, TPC1, and an anaplastic thyroid carcinoma cell line, 8505c, to stably express PROX1, along with their respective control cells (termed TPC1-Ctr, TPC1-Prx, 8505c-Ctr and 8505c-Prx) and their successful PROX1 expression were confirmed (Supplemental Fig. 4C). Like BCPAP, we observed the similar PROX1-

mediated transcriptional regulation of the abovementioned genes in these additional cells lines (Supplemental Fig. 6). Taken together, our data show that restored PROX1 activity imposes a significant impact to the transcriptional profiles of thyroid cancer cells.

Restored PROX1 activity suppresses malignant phenotypes of thyroid cancer cells

We next investigated the impact of restored PROX1 activity to thyroid cancer cell phenotypes and studied the effect of PROX1 re-expression on the single cell motility by allowing BCPAP-Ctr and BCPAP-Prx cells to migrate on the colloidal gold-covered surface in low serum media with or without Dox, and by measuring the average migration area of individual cells (Supplemental Fig. 7). Dox-induced PROX1 re-expression was found to significantly suppress BCPAP cell migration (Figure 5A). Dox treatment itself also caused a non-specific inhibition to control cell migration as previously reported (28). In addition, the scratch assays showed that PROX1 re-expression inhibited BCPAP to recover the scratched wound area (Figure 5B). Thus, the individual cell motility test and the scratch assays convincingly demonstrated that PROX1 suppressed the migratory capacity of thyroid cancer cells. Furthermore, cell adhesion assays revealed that PROX1 re-expression reduced the capability of BCPAP cells to adhere to the extracellular matrix (Figure 5C). We also found that PROX1 re-expression inhibited BCPAP cells to grow in soft agar gels and to form distinct colonies in an anchorage-independent manner, a key *in vitro* hallmark for tumor cell growth (Figure 5D). Similarly, we also verified that PROX1 re-expression inhibited the migration and adhesion of TPC1 and 8508c thyroid cancer cells (Supplemental Fig. 8A,B), indicating the consistency of PROX1 function in suppressing the aggressive behavior of various thyroid cancer cells.

We next performed the Bromodeoxyuridine (BrdU)-based cell proliferation assay to assess the effect of PROX1 re-expression on the capacity of thyroid cancer cell growth. Flow cytometry analyses detected that Dox-mediated PROX1 re-expression inhibited BrdU incorporation by 15~25% in BCPAP cells (Figure 6A). From the same set of assays, PROX1 re-expression was found to reduce the number of polyploid cells ($> 4n$) (Figure 6B). In addition, we investigated the effect of PROX1 re-expression on the invasive potential of BCPAP cells by embedding the cell spheroids in Matrigel matrix, and measuring the degree of smoothness of the leading front of the spheroid colonies. Indeed, while BCPAP cells showed sharp and jagged leading edges, PROX1 re-expression by Dox in BCPAP-Prx cells significantly suppressed these invasive phenotypes (Figure 6C,D). We also confirmed that restored PROX1 activity inhibited the cell cycle progression and polyploidy formation of TPC1 and 8505c cells (Supplemental Fig. 8C,D). Together, PROX1 re-expression suppresses various carcinoma phenotypes of thyroid cancer cells.

Reinstated PROX1 expression inhibits the *in vivo* tumor phenotypes of thyroid carcinoma cells

We next studied the effect of PROX1 re-expression on *in vivo* tumor development of thyroid cancer cells. BCPAP-Ctr or BCPAP-Prx cells were grafted into the back skin of immunodeficient NOD-SCID IL2R γ null (NSG) mice and allowed to grow with or without Dox given to the mice through drinking water. After 4 weeks, tumors were harvested and the Dox-mediated PROX1 re-expression in the tumors was confirmed by IHC (Supplemental

Fig. 9). Notably, while BCPAP-Ctr cells formed tumors with comparable size and weight regardless of Dox administration, Dox-treated, thus Prox1-expressing, BCPAP-Prx cells generated much smaller tumors than untreated BCPAP-Prx cells did (Figure 7A). Moreover, tumor histology studies revealed that tumors derived from BCPAP-Ctr cells (+/- Dox) and BCPAP-Prx cells (-Dox) demonstrated a highly invasive and aggressive cell morphology with prominently sharp and jagged tumor edges (Figure 7B). However, these typical malignant cancer characteristics were clearly suppressed in Dox-treated BCPAP-Prx tumors. In addition, Dox-treated BCPAP-Prx tumors appeared to demonstrate a lower nuclear/cytoplasmic ratio, a higher cell density and a lesser variation in size and shape of tumor cells, compared to untreated BCPAP-Prx tumors and BCPAP-Ctr tumors (+/- Dox) (Figure 7B). These findings are consistent with our *in vitro* observation of the reduced polyploid formation by PROX1 re-expression in all three thyroid cancer cell lines (Figure 6B; Supplemental Fig. 8D). Notably, Dox-mediated PROX1 induction significantly reduced the tumor cell nuclear size (Figure 7C). In addition, we also investigated the effect of PROX1 re-expression on tumor formation of TPC1 and 8505c cells by implanting TPC1-Ctr, TPC1-Prx, 8505c-Ctr and 8505c-Prx cells in NSG mice. Consistent with the BCPAP tumor phenotypes, PROX1 re-expression significantly inhibited *in vivo* tumor formation and suppressed aggressive morphological features of these two additional thyroid carcinoma cells (Supplemental Figs. 10 & 11). Together, our studies demonstrate that PROX1 re-expression significantly suppressed the aggressive *in vivo* phenotypes of thyroid cancer cells, which is consistent with the *in vitro* findings.

DISUCSSION

In this study, we demonstrated that PROX1 was inactivated by both transcriptional downregulation and protein mislocalization in various thyroid cancer cells. These initial observations brought up two important questions; (1) what are the molecular mechanisms for PROX1 downregulation and/or mislocalization and (2) what is the pathological significance of PROX1 inactivation in thyroid cancer pathogenesis? For the first question, we identified that the dysregulated NOTCH signal pathway is responsible for PROX1 mRNA downregulation in thyroid cancers, although we were unable to define the mechanism for the PROX1 mislocalization. For the second question, our *in vitro* and animal studies using multiple thyroid cancer cell lines, which were engineered to re-express PROX1, demonstrated how PROX1 inactivation could promote thyroid carcinoma development by profoundly enhancing their carcinoma phenotypes. This molecular nature of PROX1 is consistent with previous studies on the function of PROX1 in tumor development.

PROX1 has been associated with tumor development of multiple cell types. Depending on the cellular origin of the tumor cells, PROX1 either promotes or suppresses tumor incidence and behaviors. As a tumor promoter, PROX1 supports metabolic adaptation and thus enhances outgrowth of metastatic colon cancer cells with a high Wnt/ β -catenin signaling activity, and was closely correlated with a poor grade of tumor differentiation with a less favorable patient outcome (29–32). PROX1 is also upregulated in kaposiform hemangioendotheliomas and promotes their invasive phenotypes (33). In addition, PROX1 is differentially regulated in human gliomas with different malignancy grade and the

expression level is positively correlated the progression of the malignancy, suggesting that PROX1 can be useful as a diagnostic marker for different malignancy grade (34). In contrast, deletion, mutation and/or downregulation of PROX1 have been positively associated with the initiation and progression of different tumors, suggesting PROX1 to be a tumor suppressor. PROX1 was downregulated in hepatocellular carcinoma (HCC) with a poor prognosis, and ectopic expression of PROX1 in HCC cells inhibited tumor cell proliferation *in vitro* (35). Furthermore, PROX1 was found to be inactivated by downregulation, RNA mutations, genomic methylation and/or rearrangement in various tumors including hematological malignancies, breast cancer, pancreatic cancer, biliary carcinoma, esophageal and liver cancers (34).

Our study defined yet another mechanism to inactivate PROX1 activity in cancer cells, namely cytoplasmic mislocalization. PROX1 is a nuclear transcription factor with a nuclear localization signal (NLS) and principally resides in the nuclei of the normal cells. Interestingly, sequence analyses revealed that PROX1 harbors a classical nuclear export signal (NES) buried in the DNA-binding/Prospero homology domains (36–38). On the other hand, cytoplasmic localization has been reported for certain mutants of PROX1 in gastric cancer and cholangiocarcinoma (37–40). Interestingly, an antibody-based Human Protein Atlas for an expression profile study (41) found that osteosarcoma (U2OS) and rhabdomyosarcoma (RH30) show the cytoplasmic localization of PROX1 (Supplemental Fig. 12). These data have led us to hypothesize that PROX1 protein, equipped with a functional NES, may well be able to relocate to the cytoplasm by a certain signal and condition, which has not been reported to date. It will be worthwhile identifying the activating signal as well as the underlying molecular mechanism.

We found that PROX1 re-expression significantly promoted Wnt/ β -catenin signaling in thyroid cancer cells. PROX1 has previously been associated with Wnt/ β -catenin signaling in different cancer cells. Harboring TCF/LEF binding sites in its upstream region, the *PROX1* gene was found to be directly regulated by Wnt/ β -catenin signaling in colon cancer cells (29–31). More recently, PROX1 has been reported to promote HCC cell proliferation by upregulating β -catenin and enhancing its nuclear localization (42). However, we could not find evidence supporting the PROX1 regulation of β -catenin expression in thyroid cancer cells. Instead, PROX1 re-expression in thyroid cancer cells resulted in upregulation of TCF7L1 (Figure 4). Notably, a previous study searching for genome-wide PROX1 binding sites (43) revealed that PROX1 binds to immediate downstream sequences of the TCF7L1 gene and to other thyroid cancer genes, such as TC-1 and SERPINA1, which were found to be regulated by PROX1 (Figure 4). Although β -catenin protein was found in the nuclei of a large fraction of poorly and undifferentiated thyroid cancer cells, the protein was predominantly found in the cytoplasm of well-differentiated thyroid carcinoma (e.g., PTCs) (44–47), suggesting that the role of Wnt/ β -catenin signaling in thyroid cancer development may be highly variant by tumor type, stage, differentiation status and/or other tumor features. It is worth noting that the role of Wnt/ β -catenin signaling in the early stages of thyroid cancer progression and/or in well-differentiated thyroid cancer development remains a matter of debate, despite its clear roles in poorly and undifferentiated thyroid carcinoma (23).

Similarly, discussion of the expression of NOTCH pathway genes as well as the role of NOTCH signal in thyroid cancer development has been largely unsettled. However, our comparative gene expression analyses using multiple sets of clinical specimen revealed that several NOTCH pathway genes were upregulated in thyroid cancer tissues and also identified that NOTCH is responsible for PROX1 downregulation in thyroid cancer cells (Figure 2). This result is consistent with our previous finding that two prominent NOTCH effectors, HEY1 and HEY2, directly bind to the promoter area of *PROX1* gene and repress its expression (22). Consistent with our findings, NOTCH1 receptors have previously been implicated as poor prognostic markers, along with other markers such as tumor size, nodal metastasis, capsular invasion, extra thyroidal extension and lymph node metastasis (21). Moreover, kinase suppressor of RAS1 (KSR1), a scaffold protein implicated in RAS-mediated RAF activation, has recently been identified to upregulate NOTCH signal in PTC (48). Nonetheless, studies have also reported the suppressive role of NOTCH in thyroid cancer development. For example, NOTCH has been shown to suppress growth of medullary and anaplastic thyroid cancers, and activation of NOTCH signal has accordingly been proposed as a possible therapeutic approach (49,50). Therefore, more studies will be needed to clearly define the effect of NOTCH in thyroid cancer development.

In closing, our study defined the pathological significance of PROX1 inactivation in malignant behavior of thyroid carcinoma cells. Based on our findings, we propose that PROX1 inactivation may present an important prerequisite event for thyroid cancer initiation and/or progression and, accordingly, reactivation of PROX1 could be considered a therapeutic approach to possibly intervene thyroid cancer progression. In future, it will be exciting to better understand the mechanism underlying PROX1 protein mislocalization, contribution of TGF- β signal to PROX1 downregulation, the effect of thyroid hormone in PROX1 expression and the role of PROX1 in the organogenesis and physiological functions of thyroid gland.

Supplementary Material

Refer to Web version on PubMed Central for supplementary material.

Acknowledgments

This study was supported by grants from American Cancer Society (YH), American Heart Association (YH) and National Institutes of Health/National Heart Lung and Blood Institute (YH), and in part by the National Cancer Institute (P30CA014089).

REFERENCES

1. Kim WB. A closer look at papillary thyroid carcinoma. *Endocrinol Metab (Seoul)*. 2015; 30(1):1–6. [PubMed: 25827451]
2. Weber R, Bertoni AP, Bessestil LW, Brum IS, Furlanetto TW. Decreased Expression of GPER1 Gene and Protein in Goiter. *Int J Endocrinol*. 2015; 2015:869431. [PubMed: 25861267]
3. Sasaki K, Adachi S, Yamamoto T, Murakami T, Tanaka K, Takahashi M. Effects of denaturation with HCl on the immunological staining of bromodeoxyuridine incorporated into DNA. *Cytometry*. 1988; 9(1):93–96. [PubMed: 2457476]

4. Li W, Fan J, Chen M, Guan S, Sawcer D, Bokoch GM, et al. Mechanism of human dermal fibroblast migration driven by type I collagen and platelet-derived growth factor-BB. *Mol Biol Cell*. 2004; 15(1):294–309. [PubMed: 14595114]
5. Choi I, Lee S, Kyoung Chung H, Suk Lee Y, Eui Kim K, Choi D, et al. 9-cis retinoic Acid promotes lymphangiogenesis and enhances lymphatic vessel regeneration: therapeutic implications of 9-cis retinoic Acid for secondary lymphedema. *Circulation*. 2012; 125(7):872–882. [PubMed: 22275501]
6. Alajati A, Laib AM, Weber H, Boos AM, Bartol A, Ikenberg K, et al. Spheroid-based engineering of a human vasculature in mice. *Nat Methods*. 2008; 5(5):439–445. [PubMed: 18391960]
7. Cao X, Geradts J, Dewhirst MW, Lo HW. Upregulation of VEGF-A and CD24 gene expression by the tGLI1 transcription factor contributes to the aggressive behavior of breast cancer cells. *Oncogene*. 2012; 31(1):104–115. [PubMed: 21666711]
8. Rhodes DR, Yu J, Shanker K, Deshpande N, Varambally R, Ghosh D, et al. ONCOMINE: a cancer microarray database and integrated data-mining platform. *Neoplasia*. 2004; 6(1):1–6. [PubMed: 15068665]
9. Kupersmidt I, Su QJ, Grewal A, Sundaresh S, Halperin I, Flynn J, et al. Ontology-based meta-analysis of global collections of high-throughput public data. *PLoS One*. 2010; 5(9)
10. Aguilar B, Choi I, Choi D, Chung HK, Lee S, Yoo J, et al. Lymphatic reprogramming by Kaposi sarcoma herpes virus promotes the oncogenic activity of the virus-encoded G-protein-coupled receptor. *Cancer Res*. 2012; 72(22):5833–5842. [PubMed: 22942256]
11. Giordano TJ, Au AY, Kuick R, Thomas DG, Rhodes DR, Wilhelm KG Jr, et al. Delineation, functional validation, and bioinformatic evaluation of gene expression in thyroid follicular carcinomas with the PAX8-PPARG translocation. *Clin Cancer Res*. 2006; 12(7 Pt 1):1983–1993. [PubMed: 16609007]
12. Vasko V, Espinosa AV, Scouten W, He H, Auer H, Liyanarachchi S, et al. Gene expression and functional evidence of epithelial-to-mesenchymal transition in papillary thyroid carcinoma invasion. *Proc Natl Acad Sci U S A*. 2007; 104(8):2803–2808. [PubMed: 17296934]
13. Tomas G, Tarabichi M, Gacquer D, Hebrant A, Dom G, Dumont JE, et al. A general method to derive robust organ-specific gene expression-based differentiation indices: application to thyroid cancer diagnostic. *Oncogene*. 2012; 31(41):4490–4498. [PubMed: 22266856]
14. Detours V, Versteyhe S, Dumont JE, Maenhaut C. Gene expression profiles of post-Chernobyl thyroid cancers. *Curr Opin Endocrinol Diabetes Obes*. 2008; 15(5):440–445. [PubMed: 18769217]
15. Dom G, Tarabichi M, Unger K, Thomas G, Oczko-Wojciechowska M, Bogdanova T, et al. A gene expression signature distinguishes normal tissues of sporadic and radiation-induced papillary thyroid carcinomas. *Br J Cancer*. 2012; 107(6):994–1000. [PubMed: 22828612]
16. Pita JM, Banito A, Cavaco BM, Leite V. Gene expression profiling associated with the progression to poorly differentiated thyroid carcinomas. *Br J Cancer*. 2009; 101(10):1782–1791. [PubMed: 19809427]
17. Giordano TJ, Kuick R, Thomas DG, Misek DE, Vinco M, Sanders D, et al. Molecular classification of papillary thyroid carcinoma: distinct BRAF, RAS, and RET/PTC mutation-specific gene expression profiles discovered by DNA microarray analysis. *Oncogene*. 2005; 24(44):6646–6656. [PubMed: 16007166]
18. He H, Jazdzewski K, Li W, Liyanarachchi S, Nagy R, Volinia S, et al. The role of microRNA genes in papillary thyroid carcinoma. *Proc Natl Acad Sci U S A*. 2005; 102(52):19075–19080. [PubMed: 16365291]
19. Geers C, Colin IM, Gerard AC. Delta-like 4/Notch pathway is differentially regulated in benign and malignant thyroid tissues. *Thyroid*. 2011; 21(12):1323–1330. [PubMed: 22066479]
20. Yamashita AS, Geraldo MV, Fuziwara CS, Kulcsar MA, Friguglietti CU, da Costa RB, et al. Notch pathway is activated by MAPK signaling and influences papillary thyroid cancer proliferation. *Transl Oncol*. 2013; 6(2):197–205. [PubMed: 23544172]
21. Park HS, Jung CK, Lee SH, Chae BJ, Lim DJ, Park WC, et al. Notch1 receptor as a marker of lymph node metastases in papillary thyroid cancer. *Cancer Sci*. 2012; 103(2):305–309. [PubMed: 22118425]

22. Kang J, Yoo J, Lee S, Tang W, Aguilar B, Ramu S, et al. An exquisite cross-control mechanism among endothelial cell fate regulators directs the plasticity and heterogeneity of lymphatic endothelial cells. *Blood*. 2010; 116(1):140–150. [PubMed: 20351309]
23. Sastre-Perona A, Santisteban P. Role of the wnt pathway in thyroid cancer. *Front Endocrinol (Lausanne)*. 2012; 3:31. [PubMed: 22645520]
24. Chua EL, Young L, Wu WM, Turtle JR, Dong Q. Cloning of TC-1 (C8orf4), a novel gene found to be overexpressed in thyroid cancer. *Genomics*. 2000; 69(3):342–347. [PubMed: 11056052]
25. Sunde M, McGrath KC, Young L, Matthews JM, Chua EL, Mackay JP, et al. TC-1 is a novel tumorigenic and natively disordered protein associated with thyroid cancer. *Cancer Res*. 2004; 64(8):2766–2773. [PubMed: 15087392]
26. Wang YD, Bian GH, Lv XY, Zheng R, Sun H, Zhang Z, et al. TC1 (C8orf4) is involved in ERK1/2 pathway-regulated G(1)- to S-phase transition. *BMB Rep*. 2008; 41(10):733–738. [PubMed: 18959821]
27. Griffith OL, Melck A, Jones SJ, Wiseman SM. Meta-analysis and meta-review of thyroid cancer gene expression profiling studies identifies important diagnostic biomarkers. *J Clin Oncol*. 2006; 24(31):5043–5051. [PubMed: 17075124]
28. Sun T, Zhao N, Ni CS, Zhao XL, Zhang WZ, Su X, et al. Doxycycline inhibits the adhesion and migration of melanoma cells by inhibiting the expression and phosphorylation of focal adhesion kinase (FAK). *Cancer Lett*. 2009; 285(2):141–150. [PubMed: 19482420]
29. Petrova TV, Nykanen A, Norrmen C, Ivanov KI, Andersson LC, Haglund C, et al. Transcription factor PROX1 induces colon cancer progression by promoting the transition from benign to highly dysplastic phenotype. *Cancer Cell*. 2008; 13(5):407–419. [PubMed: 18455124]
30. Ragusa S, Cheng J, Ivanov KI, Zangger N, Ceteci F, Bernier-Latmani J, et al. PROX1 promotes metabolic adaptation and fuels outgrowth of Wnt(high) metastatic colon cancer cells. *Cell Rep*. 2014; 8(6):1957–1973. [PubMed: 25242332]
31. Wiener Z, Hogstrom J, Hyvonen V, Band AM, Kallio P, Holopainen T, et al. Prox1 promotes expansion of the colorectal cancer stem cell population to fuel tumor growth and ischemia resistance. *Cell Rep*. 2014; 8(6):1943–1956. [PubMed: 25242330]
32. Skog M, Bono P, Lundin M, Lundin J, Louhimo J, Linder N, et al. Expression and prognostic value of transcription factor PROX1 in colorectal cancer. *Br J Cancer*. 2011; 105(9):1346–1351. [PubMed: 21970873]
33. Dadras SS, Skrzypek A, Nguyen L, Shin JW, Schulz MM, Arbiser J, et al. Prox-1 Promotes Invasion of Kaposiform Hemangioendotheliomas. *J Invest Dermatol*. 2008
34. Elsir T, Smits A, Lindstrom MS, Nister M. Transcription factor PROX1: its role in development and cancer. *Cancer Metastasis Rev*. 2012; 31(3–4):793–805. [PubMed: 22733308]
35. Shimoda M, Takahashi M, Yoshimoto T, Kono T, Ikai I, Kubo H. A homeobox protein, prox1, is involved in the differentiation, proliferation, and prognosis in hepatocellular carcinoma. *Clin Cancer Res*. 2006; 12(20 Pt 1):6005–6011. [PubMed: 17062673]
36. Hong YK, Detmar M. Prox1, master regulator of the lymphatic vasculature phenotype. *Cell Tissue Res*. 2003
37. Baxter SA, Cheung DY, Bocangel P, Kim HK, Herbert K, Douville JM, et al. Regulation of the lymphatic endothelial cell cycle by the PROX1 homeodomain protein. *Biochim Biophys Acta*. 2011; 1813(1):201–212. [PubMed: 21040746]
38. Takeda Y, Jetten AM. Prospero-related homeobox 1 (Prox1) functions as a novel modulator of retinoic acid-related orphan receptors alpha- and gamma-mediated transactivation. *Nucleic Acids Res*. 2013; 41(14):6992–7008. [PubMed: 23723244]
39. Taban O, Cimpean AM, Raica M, Olariu S. PROX1 expression in gastric cancer: from hypothesis to evidence. *Anticancer Res*. 2014; 34(7):3439–3446. [PubMed: 24982352]
40. Laerm A, Helmbold P, Goldberg M, Dammann R, Holzhausen HJ, Ballhausen WG. Prospero-related homeobox 1 (PROX1) is frequently inactivated by genomic deletions and epigenetic silencing in carcinomas of the biliary system. *J Hepatol*. 2007; 46(1):89–97. [PubMed: 17069925]
41. Berglund L, Bjorling E, Oksvold P, Fagerberg L, Asplund A, Szigartyo CA, et al. A gene-centric Human Protein Atlas for expression profiles based on antibodies. *Mol Cell Proteomics*. 2008; 7(10):2019–2027. [PubMed: 18669619]

42. Liu Y, Ye X, Zhang JB, Ouyang H, Shen Z, Wu Y, et al. PROX1 promotes hepatocellular carcinoma proliferation and sorafenib resistance by enhancing beta-catenin expression and nuclear translocation. *Oncogene*. 2015
43. Charest-Marcotte A, Dufour CR, Wilson BJ, Tremblay AM, Eichner LJ, Arlow DH, et al. The homeobox protein Prox1 is a negative modulator of ERR{alpha}/PGC-1{alpha} bioenergetic functions. *Genes Dev*. 2010; 24(6):537–542. [PubMed: 20194433]
44. Rezk S, Brynes RK, Nelson V, Thein M, Patwardhan N, Fischer A, et al. beta-Catenin expression in thyroid follicular lesions: potential role in nuclear envelope changes in papillary carcinomas. *Endocr Pathol*. 2004; 15(4):329–337. [PubMed: 15681857]
45. Meirmanov S, Nakashima M, Kondo H, Matsufuji R, Takamura N, Ishigaki K, et al. Correlation of cytoplasmic beta-catenin and cyclin D1 overexpression during thyroid carcinogenesis around Semipalatinsk nuclear test site. *Thyroid*. 2003; 13(6):537–545. [PubMed: 12930597]
46. Ishigaki K, Namba H, Nakashima M, Nakayama T, Mitsutake N, Hayashi T, et al. Aberrant localization of beta-catenin correlates with overexpression of its target gene in human papillary thyroid cancer. *J Clin Endocrinol Metab*. 2002; 87(7):3433–3440. [PubMed: 12107263]
47. Garcia-Rostan G, Camp RL, Herrero A, Carcangiu ML, Rimm DL, Tallini G. Beta-catenin dysregulation in thyroid neoplasms: down-regulation, aberrant nuclear expression, and CTNNB1 exon 3 mutations are markers for aggressive tumor phenotypes and poor prognosis. *Am J Pathol*. 2001; 158(3):987–996. [PubMed: 11238046]
48. Lee J, Seol MY, Jeong S, Kwon HJ, Lee CR, Ku CR, et al. KSR1 is coordinately regulated with Notch signaling and oxidative phosphorylation in thyroid cancer. *J Mol Endocrinol*. 2015; 54(2): 115–124. [PubMed: 25608512]
49. Ferretti E, Tosi E, Po A, Scipioni A, Morisi R, Espinola MS, et al. Notch signaling is involved in expression of thyrocyte differentiation markers and is down-regulated in thyroid tumors. *J Clin Endocrinol Metab*. 2008; 93(10):4080–4087. [PubMed: 18664540]
50. Cook M, Yu XM, Chen H. Notch in the development of thyroid C-cells and the treatment of medullary thyroid cancer. *Am J Transl Res*. 2010; 2(1):119–125. [PubMed: 20182588]

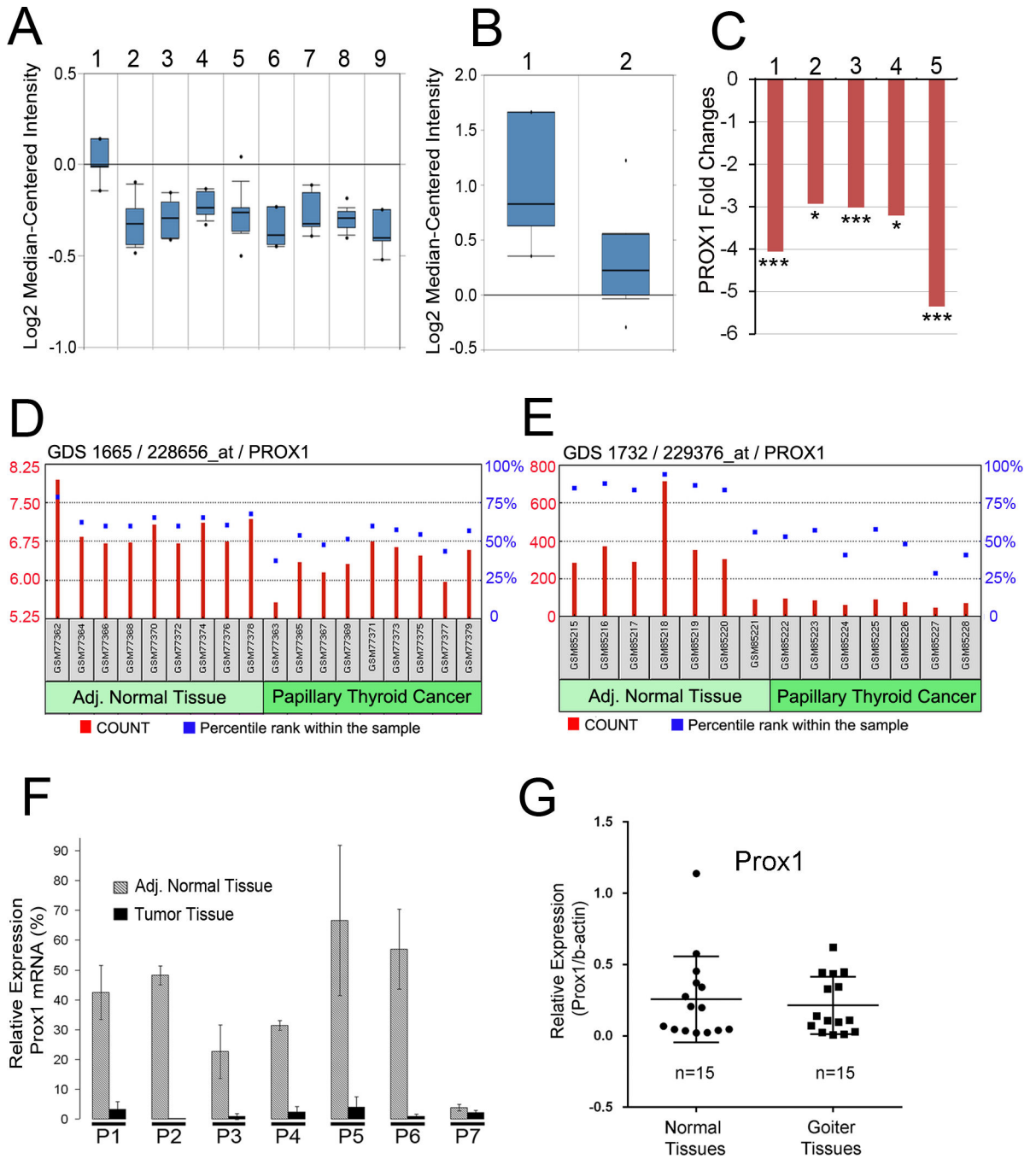


Figure 1. Downregulation of PROX1 in various thyroid cancers

(A) PROX1 expression in normal thyroid tissues vs. thyroid cancers (n=97). Lane 1, Normal thyroid gland (n=4); Lane 2, Follicular variant PTC (n=15); Lane 3, Tall cell variant PTC (n=10); Lane 4, Follicular adenoma (n=10); Lane 5, Follicular carcinoma (n=13); Lane 6, Oncocytic adenoma (n=7); Lane 7, Oncocytic follicular carcinoma (n=8); Lane 8, PTC (n=26); Lane 9, Undifferentiated (anaplastic) carcinoma (n=4). Data source: GSE27155 (11). (B) PROX1 expression in normal thyroid gland (Lane 1, n=4) vs. PTC (Lane 2, n=14). Data source: GSE6004 (12). (C) Fold changes in PROX1 expression in thyroid cancers vs.

normal tissues. PTC (Lane 1), Chernobyl accident PTC (Lane 2), Sporadic (no radiation exposure) PTC (Lane 3), Classic PTC with BRAF V600E mutation (Lane 4), Thyroid carcinomas from The Cancer Genome Atlas (TCGA) patients (Lane 5). Data source: GSE33630, GSE29265, GSE29265, GSE53157 and TCGA. **(D,E)** PROX1 levels in PTC and their adjacent (Adj.) normal thyroid glands are visualized by relative probe intensities (count) and percentile ranks (%) in two GEO data sets (GSE3467, GSE3678) (18). **(F)** qRT-PCR was performed to verify PROX1 levels in PTC and adjacent normal thyroid glands (GSE3678). *PROX1* mRNA level was normalized against the expression of *GAPDH* mRNA. **(G)** qRT-PCR data showing relative expressions of PROX1 in normal vs. goiter samples after normalization against *ACTB* mRNA. Error bars present standard deviations. *, $p < 0.05$; **, $p < 0.01$; ***, $p < 0.001$. Detailed information on the data sets is summarized in Supplemental Table 1.

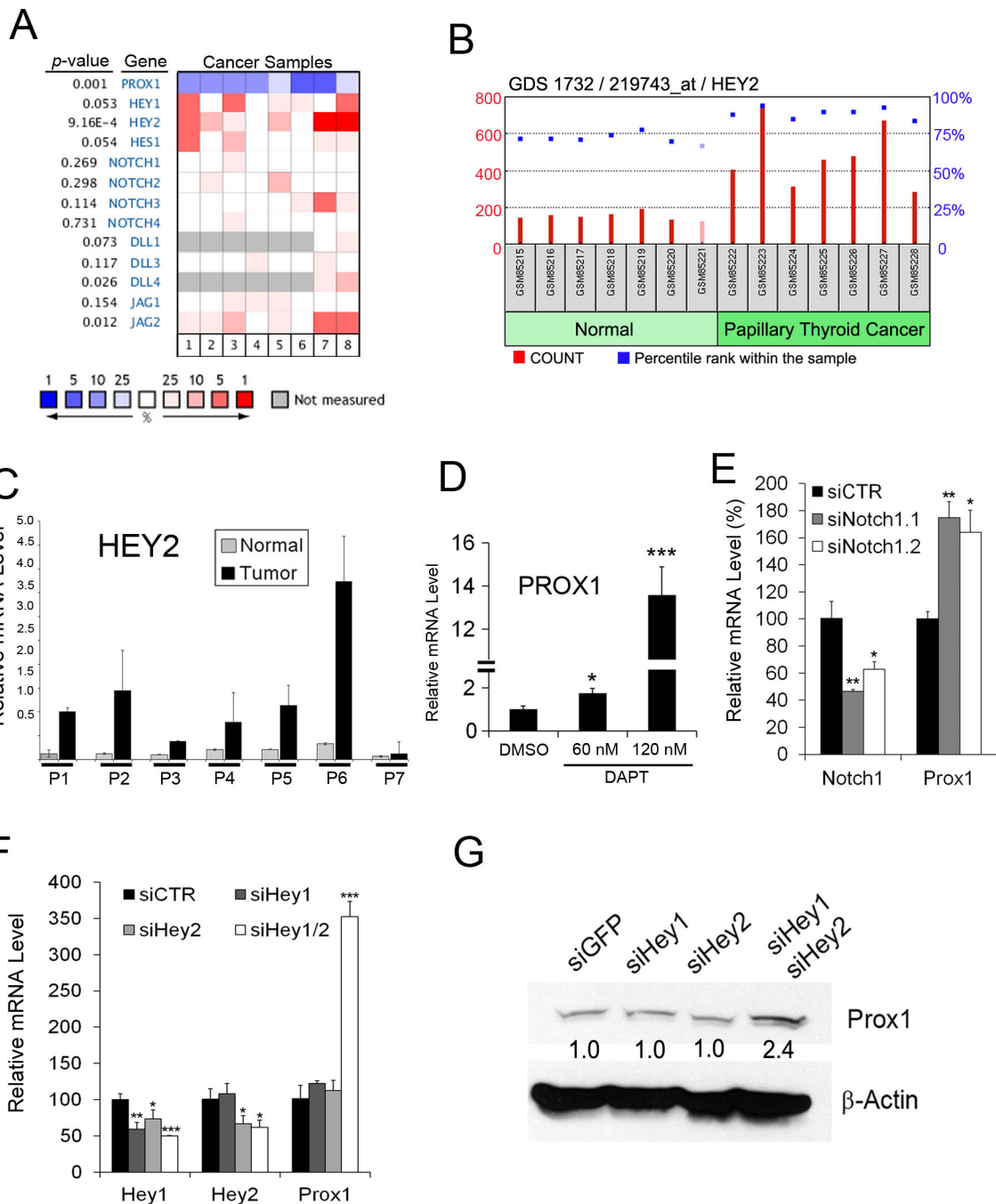


Figure 2. NOTCH is responsible for PROX1 downregulation in thyroid cancers

(A) Heat map showing expression of NOTCH genes in the following thyroid cancers, compared to normal thyroid tissues. Lane 1, follicular variant PTC (11); Lane 2, tall cell variant PTC (11); Lane 3, follicular carcinoma (11); Lane 4, oncocyctic follicular carcinoma (11); Lane 5, PTC (11); Lane 6, undifferentiated (anaplastic) carcinoma (11); Lane 7, PTC (18); Lane 8, PTC (12). Heat map represents the median percentile rank for a given gene across each of the analyses. Data source: GSE27155 (11) (B) *HEY2* mRNA levels were determined in seven PTC vs. their paired normal tissues, and displayed for relative probe

intensities (count) and percentile ranks (%) within the sample. Data source: GSE3678. (C) qRT-PCR assays showing *HEY2* mRNA levels in the normal vs. tumor samples of panel (B). (D,E) NOTCH Inhibition in BCPAP cells using DAPT (60 and 120 nM) (D) or two different siRNAs against NOTCH1 (E) for 48 hours resulted in PROX1 upregulation in BCPAP. (F,G) HEY1 and HEY2 synergistically downregulate PROX1. Expressions of HEY1 and/or HEY2 were inhibited by their corresponding siRNA in BCPAP cells (F) and TPC1 cells (G). After 48 hours, PROX1 expression was determined by qRT-PCR (F) or western blot (G) analyses. Error bars present standard deviations. *, $p < 0.05$; **, $p < 0.01$; ***, $p < 0.001$.

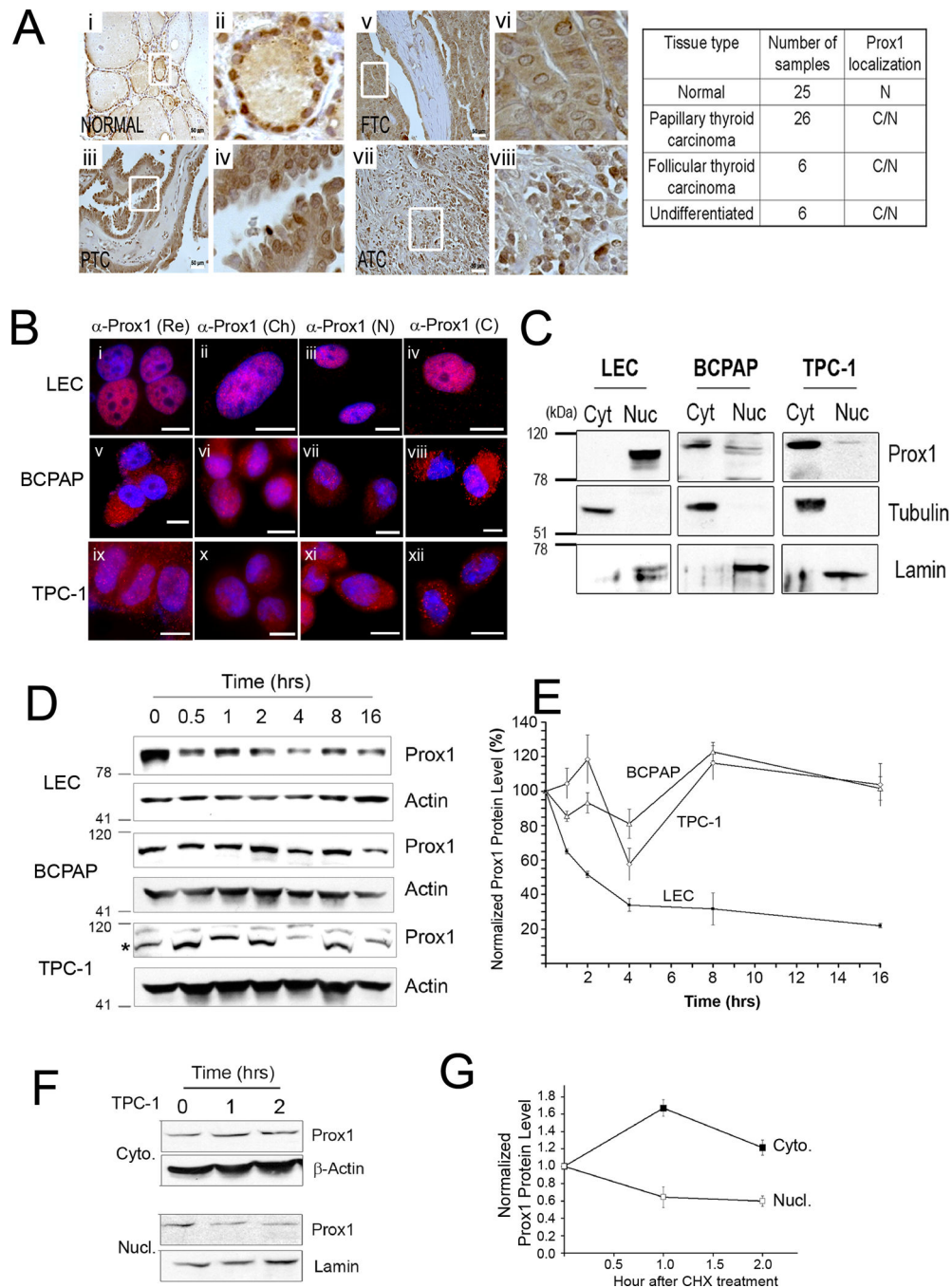


Figure 3. PROX1 protein is mislocalized to the cytoplasm and gains enhanced protein stability in thyroid cancer cells

(A) IHC showing PROX1 localization in normal thyroid tissues (Normal, n=25), PTC (n=26), follicular thyroid carcinoma (FTC, n=6), anaplastic or undifferentiated thyroid carcinoma (ATC, n=6). Overview (i, iii, v, vii) are shown with enlarged images (ii, iv, vi, viii). Scale bars, 50 μ m. PROX1 localization: nuclei (N), cytoplasm (C). (B) IF analyses showing PROX1 localization in LECs (i–iv), BCPAP (v–viii) and TPC1 (ix–xii). Four different PROX1 antibodies were used: rabbit polyclonal antibody from Reliatech (Re)

(i,v,ix), mouse monoclonal antibody 5G10 from Millipore (Ch) (ii,vi,x), custom generated rabbit polyclonal antibodies against PROX1 N-terminus (N) (iii, vii,xi) and C-terminus (C) (iv,viii,xii). PROX1 was stained in red and the nuclei with DAPI. Scale Bars, 20 μm . (C) Western blot assays showing subcellular distribution of PROX1 protein. The cytoplasmic (cyt) and nuclear (nuc) fractions were obtained from LEC, BCPAP and TPC1, and probed for PROX1. Tubulin and lamin were also detected as the controls for the cytoplasmic and nuclear fractions, respectively. (D,E) PROX1 protein is more stable in PTC cells than in LECs. LECs, BCPAP and TPC1 cells were treated with cycloheximide (100 $\mu\text{g}/\text{ml}$) for the indicated time. Western blot analyses showing PROX1 protein (D). PROX1 band is marked with an asterisk for TPC-1 blot. PROX1 expression was normalized against β -actin (E). (F,G) Cytoplasmic PROX1 protein is more stable than nuclear PROX1. TPC1 cells were treated with cycloheximide (100 $\mu\text{g}/\text{ml}$) for 0, 1 and 2 hours, followed by subcellular fractionation. Western blotting for PROX1 in the cytoplasmic (Cyto.) and nuclear (Nucl.) fractions (F). β -actin and lamin were also detected as the controls for the cytoplasmic and nuclear fractions, respectively. Normalized band intensities of the cytoplasmic and nuclear PROX1 proteins to β -actin and lamin proteins, respectively (G). Error bars present standard deviations.

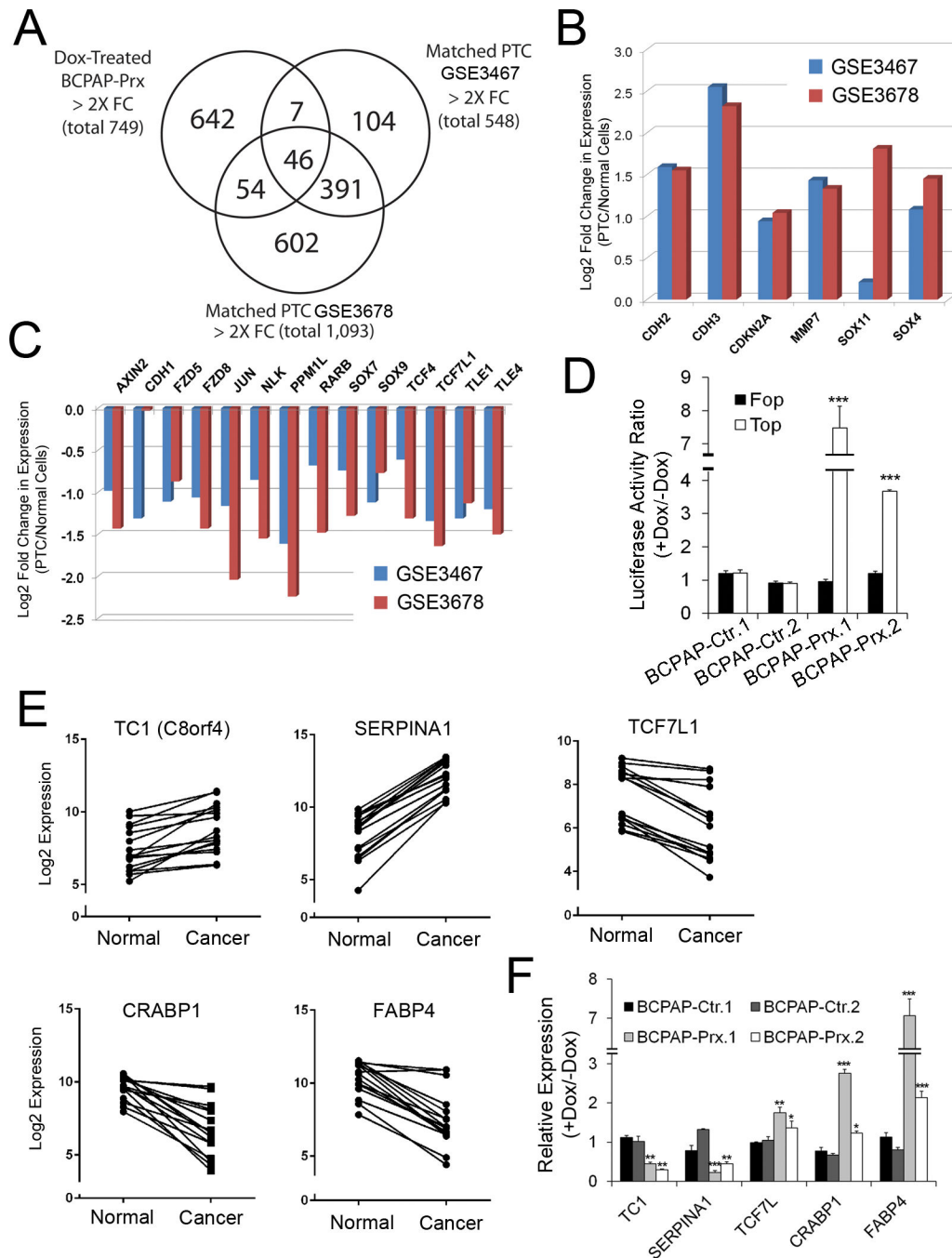


Figure 4. Profound impact of PROX1 activity to the transcriptional profiles of thyroid cancer cells

(A) Venn diagram showing that PROX1 regulates approximately 10% of differentially regulated genes in the normal tissues *vs.* matched PTC. Genes with > 2-fold changes were selected in each data base. (B,C) IPA-based analyses identified Wnt/β-catenin signaling as a key pathway that was suppressed in PTC tissues from two independent PTC expression studies (GSE3467, GSE3678). Genes that were previously associated with Wnt/β-catenin signaling are listed with their expression changes. (D) PROX1 re-expression enhances the

activity of Wnt/ β -catenin signaling in BCPAP cells. The β -catenin activity reporter vector (TOP-Flash) or its mutant control vector (FOP-Flash) was transfected for 12 hours and the cells were treated with or without Dox for 36 hours. **(E,F)** Examples of genes are listed whose expression was consistently changed in PTC tissues **(E)** Expression of these genes was correspondingly regulated by PROX1 re-expression in BCPAP cells **(F)**. Error bars present standard deviations. *, $p < 0.05$; **, $p < 0.01$; ***, $p < 0.001$.

Author Manuscript

Author Manuscript

Author Manuscript

Author Manuscript

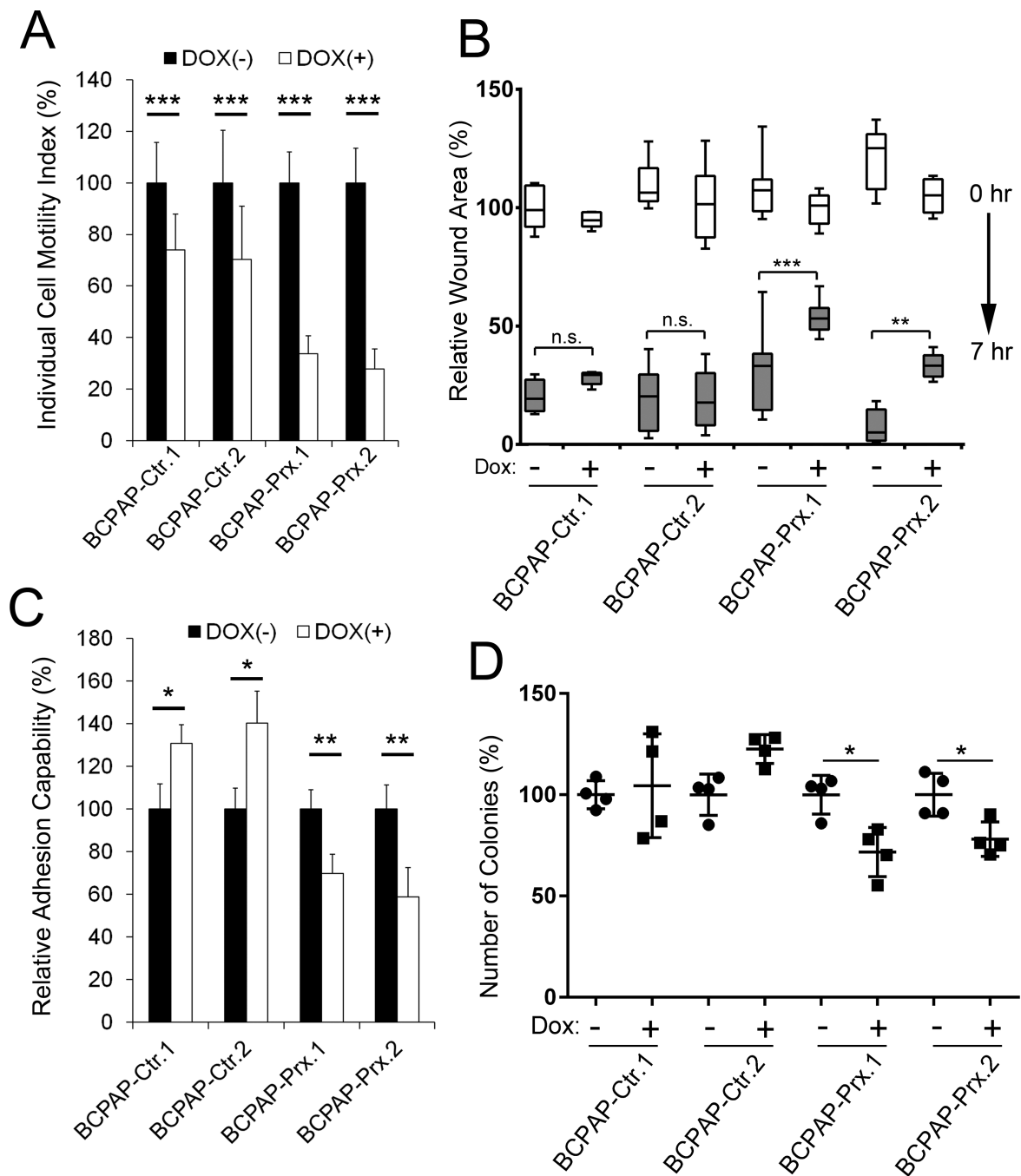


Figure 5. Restored PROX1 activity suppresses motility, adhesion and anchorage-independent growth of thyroid cancer cells

(A) Suppressed motility of BCPAP cells by Dox-mediated PROX1 re-expression. Motility of individual cells ($n > 20$) was measured on colloidal gold-covered surface in a low serum media with or without Dox for 16 hours. Average migrated areas were determined and displayed as percent cell motility. (B) Delayed recovery of scratched wounds upon PROX1 expression in BCPAP cells. Scratched wounds were made on monolayer of BCPAP-Ctr or BCPAP-Prx cells, and allowed to be recovered for 7 hours in the presence or absence of

Dox. Relative wounds area was measured at 0 hour (white box) and after 7 hours (gray box). **(C)** PROX1 re-expression suppressed BCPAP cell adhesion to extracellular matrix. BCPAP-Ctr or BCPAP-Prx cells, cultured in the media with or without Dox, were allowed to adhere to culture plates pre-coated with extracellular matrix mixture (collagen, fibronectin and gelatin) and followed by gentle washing. Number of the remaining adherent cells was analyzed. **(D)** Soft agar colony formation assay showing reduced colony formation in BCPAP cells upon Dox-mediated PROX1 re-expression. Error bars present standard deviations. *, $p < 0.05$; **, $p < 0.01$; ***, $p < 0.001$.

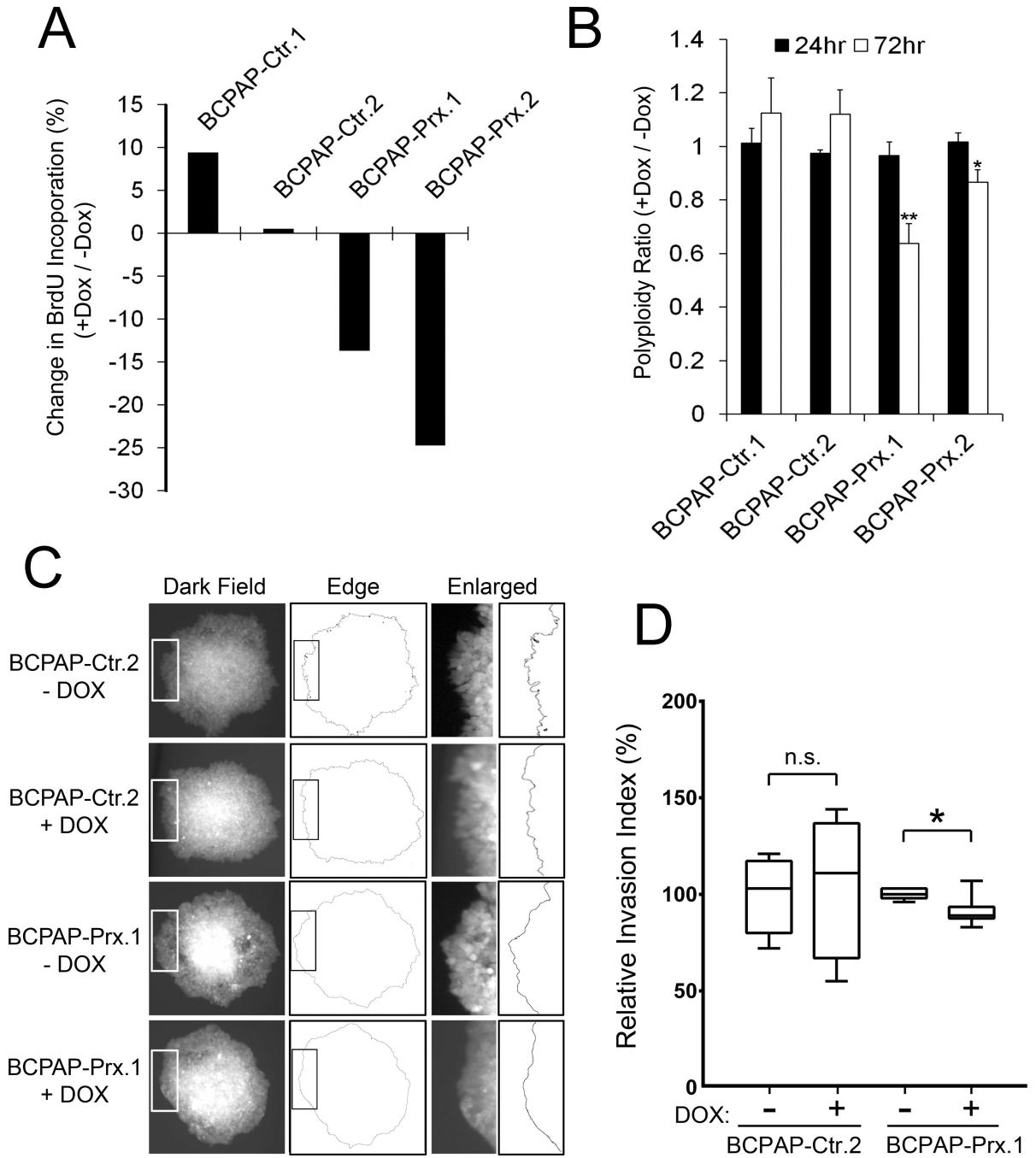


Figure 6. Re-expression of PROX1 inhibits the carcinoma behaviors of PTC cells

(A) BrdU incorporation assay showing a reduced BrdU incorporation in BCPAP cells upon Dox-mediated PROX1 re-expression. (B) Flow cytometric DNA content analysis showing a decrease in the number of cells containing more than tetraploid (4n) after Dox-mediated PROX1 re-expression in BCPAP cells. (C,D) Cell invasion assay showing that restored PROX1 activity suppressed the invasive phenotype of BCPAP cells. Cell spheroids were embedded in Matrigel matrix and cultured for 24 hours in the presence or absence of Dox. Images of the spheroid colonies on the surface of the culture plate (i.e., bottom of Matrigel)

were randomly captured and processed using NIH ImageJ (C). Relative smoothness (Invasion Index) of the invading front line of each colony was calculated as described in Supplemental Information. (D). Error bars present standard deviations. *, $p < 0.05$; **, $p < 0.01$.

Author Manuscript

Author Manuscript

Author Manuscript

Author Manuscript

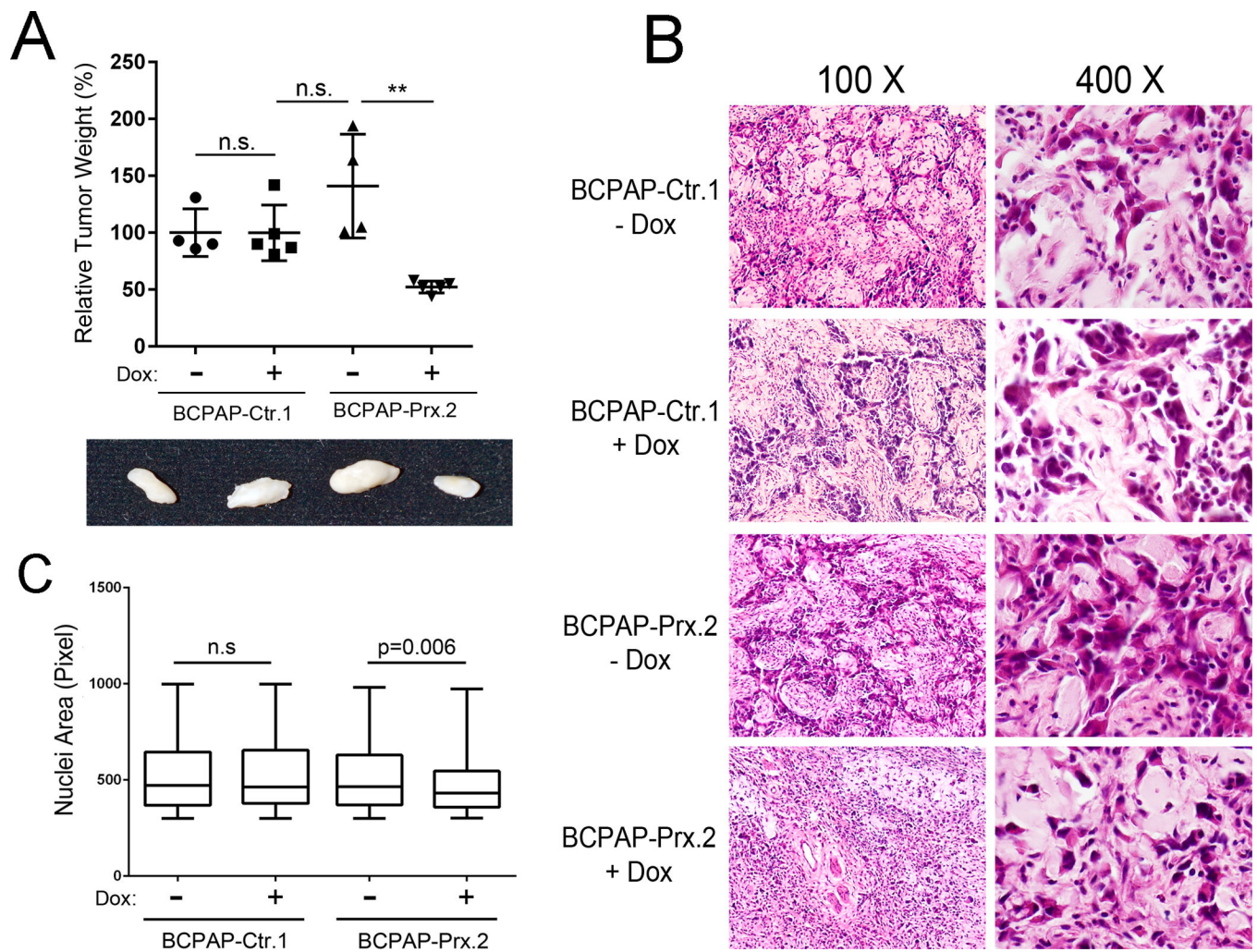


Figure 7. PROX1 re-expression suppresses the *in vivo* phenotypes of thyroid carcinoma
(A) Relative weights of tumors formed by 3 million BCPAP-Ctr and BCPAP-Prx cells that were grafted in the back skin of the immunodeficient NSG mice, which were subsequently given Dox through drinking water for 28 days. 4~5 mice were used for each group and two rounds of experiment were performed with the similar results. **, $p < 0.01$. **(B)** H&E staining images of each tumor. Note BCPAP tumor cells (darker pink) and mouse stromal cells (pale pink). **(C)** Comparative estimation of the nuclear size (in pixel) of the BCPAP tumor cells. Mean \pm SEM of each group and sample size are as follows: BCPAP-Ctr.1/-Dox (521.9 ± 9.2 , $n=400$), BCPAP-Ctr.1/+Dox (519.8 ± 9.3 , $n=369$), BCPAP-Prx.1/-Dox (515.8 ± 7.6 , $n=526$), BCPAP-Prx.1/+Dox (477.7 ± 7.2 , $n=393$).